

## Supporting Information

# Advanced Hybrid Supercapacitor Based on Mesoporous Niobium Pentoxide/Carbon as High-Performance Anode

*Eunho Lim,<sup>†, †</sup> Haegyeom Kim,<sup>§, †</sup> Changshin Jo,<sup>‡, †</sup> Jinyoung Chun,<sup>‡</sup> Kyojin Ku,<sup>§</sup> Seongseop Kim,<sup>‡</sup> Hyung Ik Lee,<sup>¥</sup> In-Sik Nam,<sup>†, ‡</sup> Songhun Yoon,<sup>‡, \*</sup> Kisuk Kang,<sup>§, □, \*</sup> and Jinwoo Lee<sup>†, ‡, \*</sup>*

<sup>†</sup>School of Environmental Science and Engineering, Pohang University of Science and Technology (POSTECH), Pohang, Kyungbuk 790-784, Republic of Korea

<sup>‡</sup>Department of Chemical Engineering, Pohang University of Science and Technology (POSTECH), Pohang, Kyungbuk 790-784, Republic of Korea

<sup>§</sup>Department of Materials Science and Engineering, Research Institute of Advanced Materials (RIAM), Seoul National University, 599 Gwanak-ro, Gwanak-gu, Seoul, Republic of Korea

<sup>¥</sup>4-3, Agency for Defense Development, Yuseong, P.O. Box 35-4, 305-600 Daejeon, Republic of Korea

<sup>‡</sup>Department of Integrative Engineering, Chung-Ang University, 221, Heukseok-Dong, Dongjak-Gu, Seoul, 156-756, Republic of Korea

<sup>‡</sup>Center for Nanoparticle Research, Institute for Basic Science (IBS), Seoul National University, Seoul 151-742, Republic of Korea

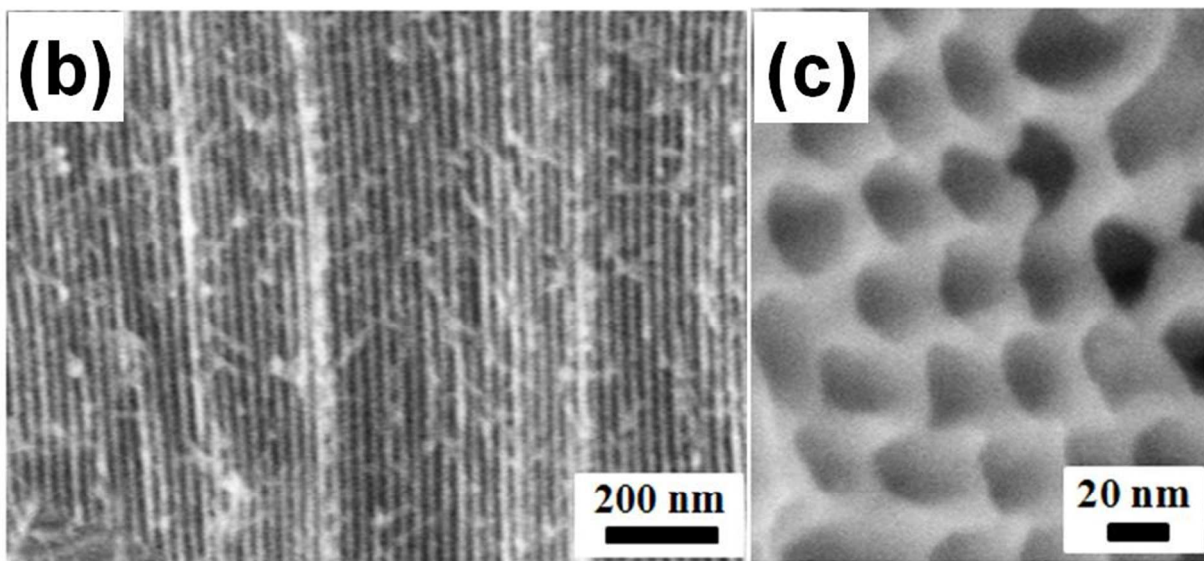
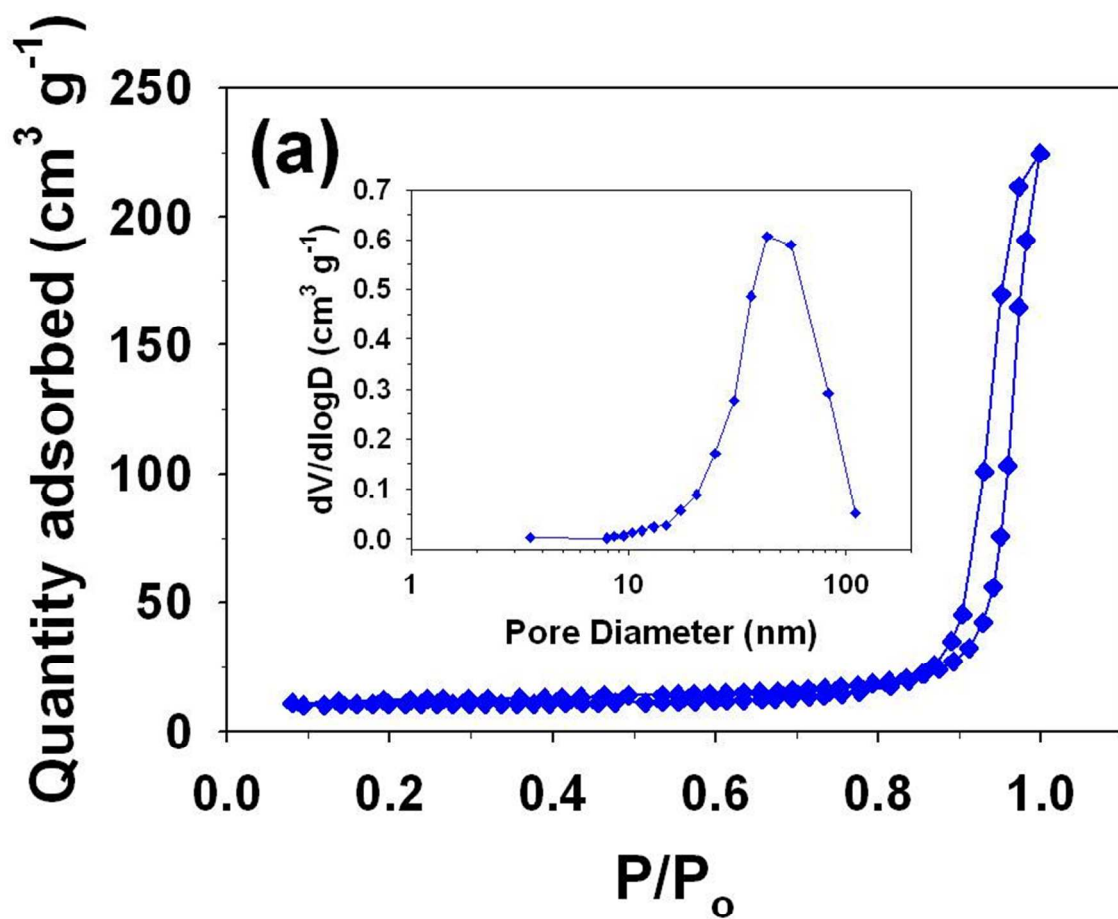


**Figure S1.** (a) N<sub>2</sub> adsorption-desorption isotherm for m-Nb<sub>2</sub>O<sub>5</sub> and the corresponding pore size distribution. SEM images of (b) as-synthesized Nb<sub>2</sub>O<sub>5</sub> and (c) m-Nb<sub>2</sub>O<sub>5</sub>.

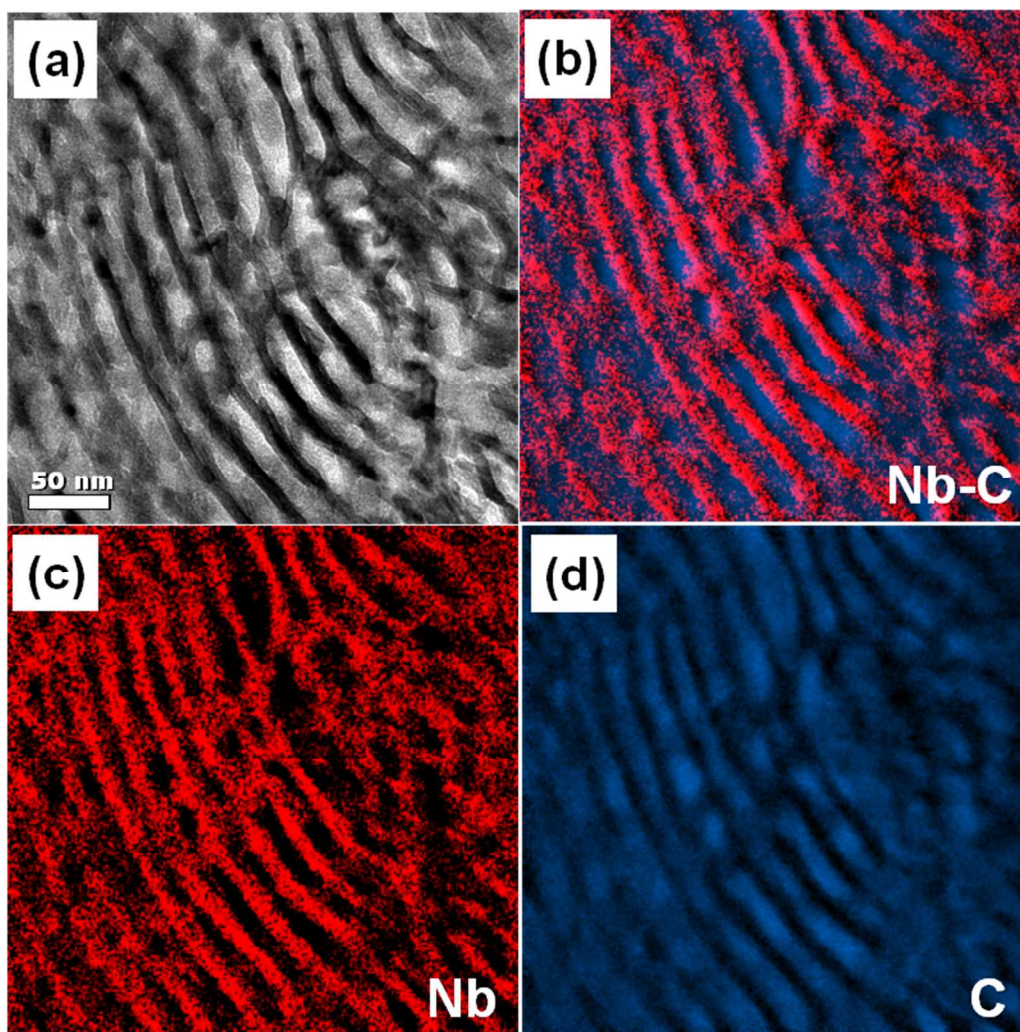


**Figure S2.** Electron microscopy images. (a) microtomed TEM image of m-Nb<sub>2</sub>O<sub>5</sub>-C (b, c, d) EELS mapping images of the (b) Nb-C, (c) Nb, and (d) C.

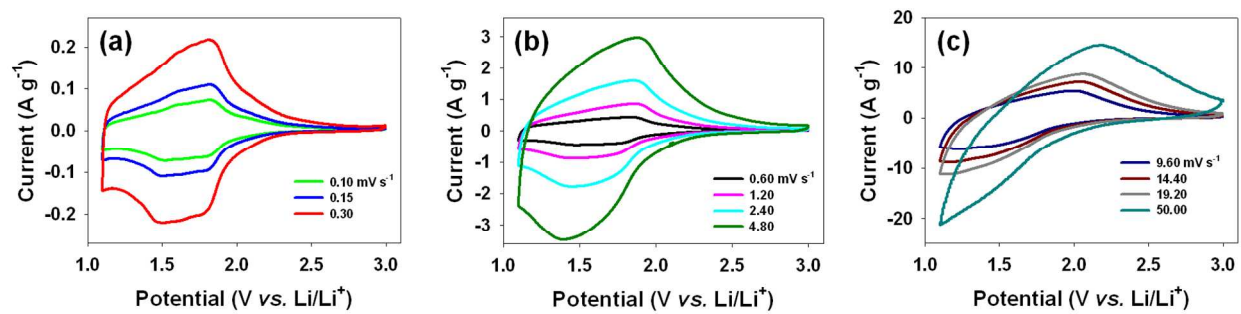


**Figure S3.** CV analysis of m-Nb<sub>2</sub>O<sub>5</sub>-C at different sweep rates (a) from 0.10 to 0.30 mV s<sup>-1</sup>, (b) from 0.60 to 4.80 mV s<sup>-1</sup>, and (c) from 9.60 to 50.00 mV s<sup>-1</sup>. The distorted CV profiles at high scan rates are inevitable due to a variety of resistances resulting from coin-type cells.

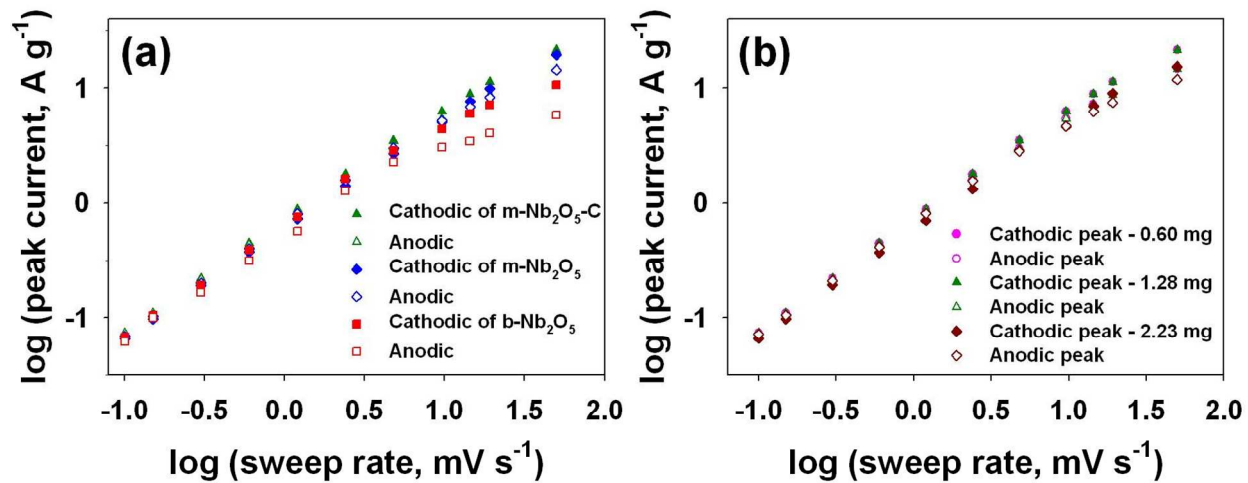


**Figure S4.** Specific peak current with respect to various sweep rates of (a) m-Nb<sub>2</sub>O<sub>5</sub>-C, m-Nb<sub>2</sub>O<sub>5</sub>, and b-Nb<sub>2</sub>O<sub>5</sub> and (b) different mass loadings of m-Nb<sub>2</sub>O<sub>5</sub>-C between 0.1 and 50 mV s<sup>-1</sup>.

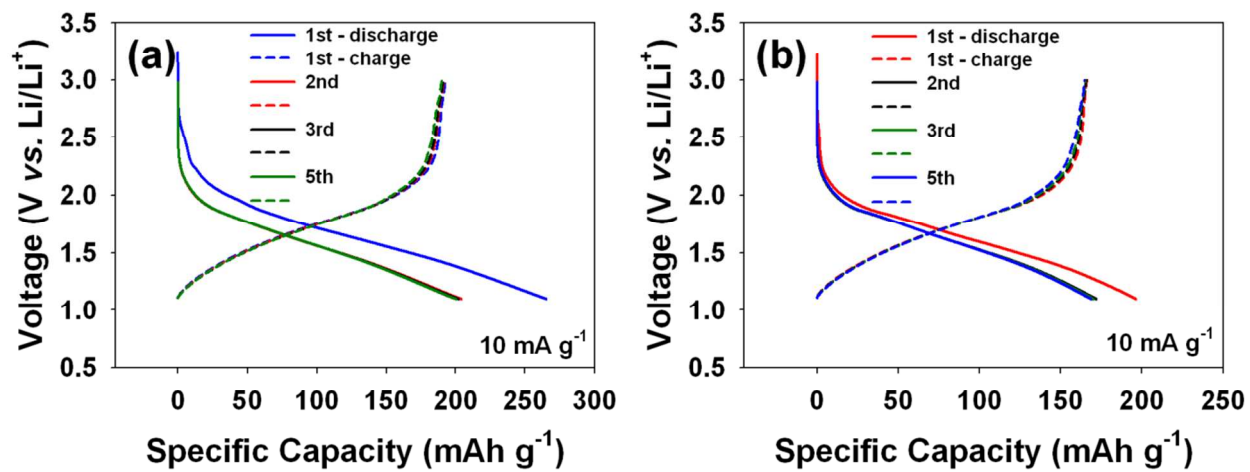


**Figure S5.** Charge-discharge voltage profiles of (a) m-Nb<sub>2</sub>O<sub>5</sub> and (b) b-Nb<sub>2</sub>O<sub>5</sub> at 10 mA g<sup>-1</sup>.

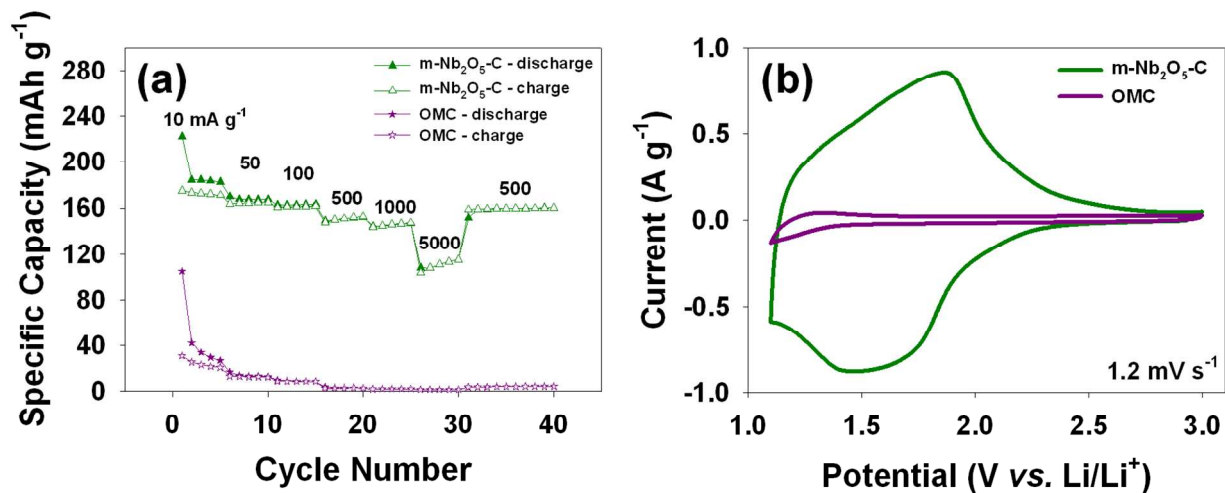


**Figure S6.** (a) Comparison of capacities of the m-Nb<sub>2</sub>O<sub>5</sub>-C/Li and ordered mesoporous carbon (OMC)/Li half cells under different current densities varying from 10 to 5000 mA g<sup>-1</sup>. (b) CV analysis at 1.2 mV s<sup>-1</sup> for the m-Nb<sub>2</sub>O<sub>5</sub>-C/Li and OMC/Li half cells (OMC, main pore size: 32 nm, specific surface area: 521 m<sup>2</sup> g<sup>-1</sup>).



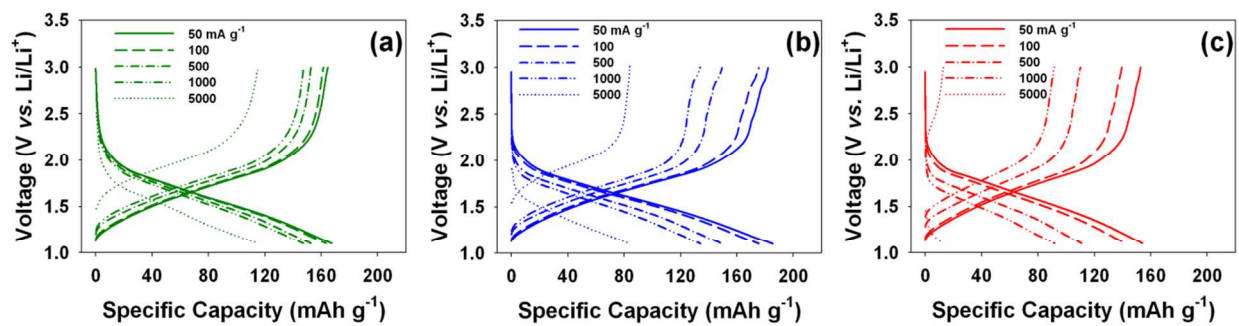


**Figure S7.** Charge-discharge voltage profiles of (a) m-Nb<sub>2</sub>O<sub>5</sub>-C, (b) m-Nb<sub>2</sub>O<sub>5</sub>, and (c) b-Nb<sub>2</sub>O<sub>5</sub> at various current densities (50 to 5000 mA g<sup>-1</sup>).

**Table S1.** The electrical conductivity of m-Nb<sub>2</sub>O<sub>5</sub>-C and m-Nb<sub>2</sub>O<sub>5</sub>.

<b>Sample</b>	<b>Electrical conductivity (S cm<sup>-1</sup>)</b>
m-Nb <sub>2</sub> O <sub>5</sub> -C	$3.49 \times 10^{-3}$
m-Nb <sub>2</sub> O <sub>5</sub>	$1.44 \times 10^{-7}$

The electrochemical conductivity was measured by using Van der Pauw four-probe methods.<sup>1</sup>

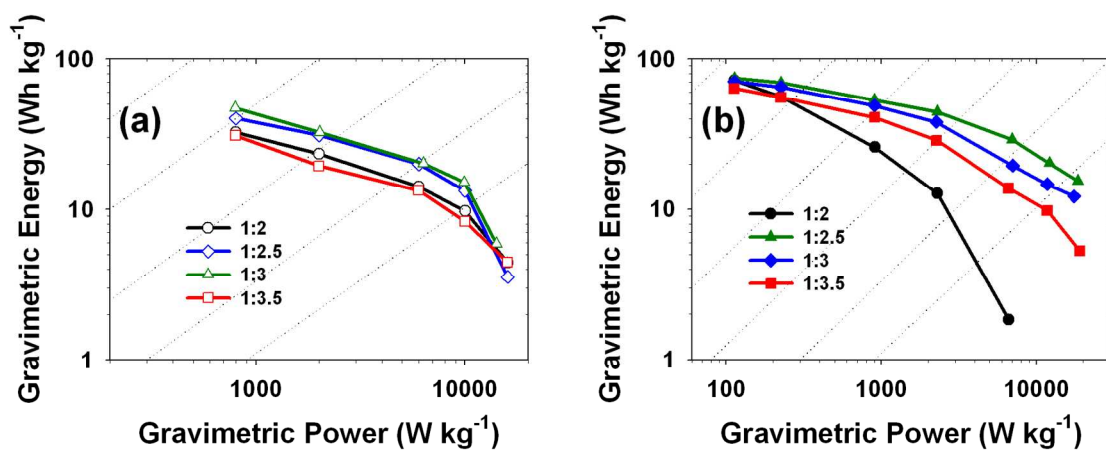


**Figure S8.** Ragone plots of hybrid supercapacitors based on m-Nb<sub>2</sub>O<sub>5</sub>-C and MSP-20 with different mass ratio of anode and cathode active materials in the voltage range of (a) 0.5-3.0 V and (b) 0.5-3.5 V.

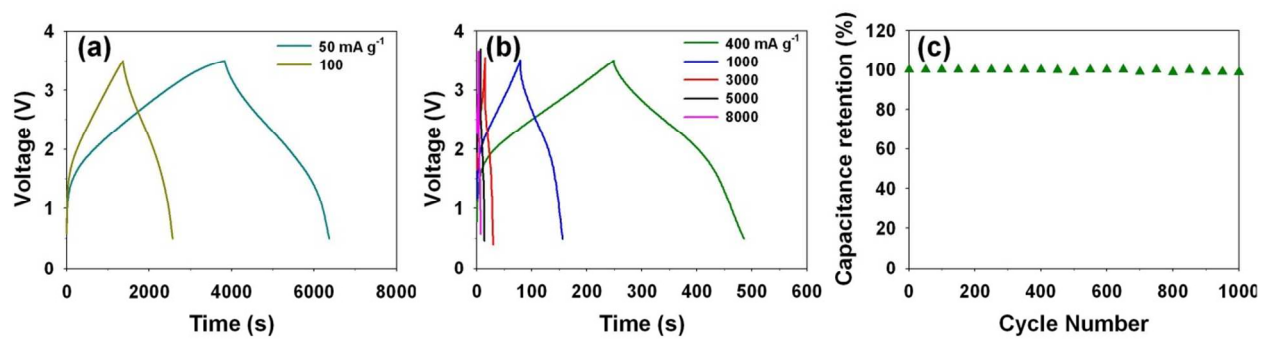


**Figure S9.** (a, b) Charge-discharge profiles of hybrid supercapacitor based on m-Nb<sub>2</sub>O<sub>5</sub>-C anode between 0.5 and 3.5 V at different current rates. (c) Cycling performance of hybrid supercapacitor based on m-Nb<sub>2</sub>O<sub>5</sub>-C anode between 0.5 and 3.5 V at a current rate of 5000 mA g<sup>-1</sup>.

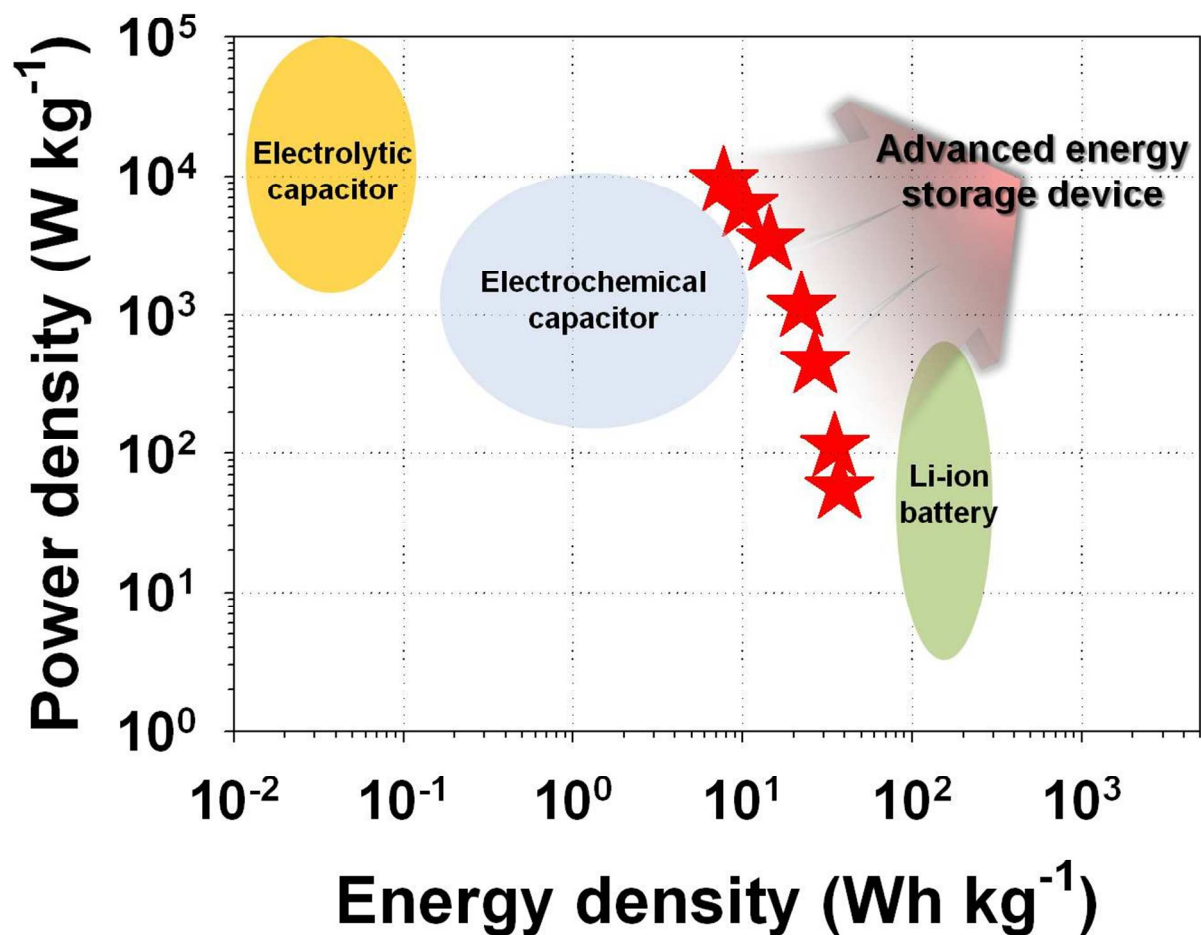


**Figure S10.** Ragone plots of commercial energy storage devices and the hybrid supercapacitor using  $m\text{-Nb}_2\text{O}_5\text{-C}$  (★). In order to consider commercialization of the hybrid supercapacitor using  $m\text{-Nb}_2\text{O}_5\text{-C}$ , the gravimetric energy and power densities of the hybrid supercapacitor using  $m\text{-Nb}_2\text{O}_5\text{-C}$  (★) were calculated by dividing the values of the energy and power densities of the electrode by a factor of 2.<sup>2-4</sup>

## REFERENCES AND NOTES

1. Kang, E.; An, S.; Yoon, S.; Kim, J. K.; Lee, J. Ordered Mesoporous  $\text{WO}_{3-x}$  Possessing Electronically Conductive Framework Comparable to Carbon Framework toward Long-Term Stable Cathode Supports for Fuel Cells. *J. Mater. Chem.* **2010**, 20, 7416-7421.
2. Dudney, N. J. Thin Film Micro-Batteries. *Electrochem. Soc. Interfaces.* **2008**, 17, 44-48.
3. Li, W.; Dahn, R. Wainwright, D. S. Rechargeable Lithium Batteries with Aqueous Electrolytes. *Science* **1994**, 264, 1115-1118.
4. Kim, H.; Cho, M.-Y.; Kim, M.-H.; Park, K.-Y.; Gwon, H.; Lee, Y.; Roh, K. C.; Kang, K. A Novel High-Energy Hybrid Supercapacitor with an Anatase  $\text{TiO}_2$ -Reduced Graphene Oxide Anode and an Activated Carbon Cathode. *Adv. Energy Mater.* **2013**, 3, 1500-1506.